Megafloods in Europe can be anticipated from observations in hydrologically similar catchments

Miriam Bertola, Günter Blöschl, Milon Bohac, Marco Borga, Attilio Castellarin, Giovanni B Chirico, Pierluigi Claps, Eleonora Dallan, Irina Danilovich, Daniele Ganora, et al.

Megafloods in Europe can be anticipated from observations in hydrologically similar catchments

Author list

Miriam Bertola[1*], Günter Blöschl[1], Milon Bohac[2], Marco Borga[3], Attilio Castellarin[4], Giovanni B. Chirico[5], Pierluigi Claps[6], Eleonora Dallan[3], Irina Danilovich[7], Daniele Ganora[6], Liudmyla Gorbachova[8], Ondrej Ledvinka[2,9], Maria Mavrova-Guirguinova[10], Alberto Montanari[4], Valeriya Ovcharuk[11], Alberto Viglione[6], Elena Volpi[12], Berit Arheimer[13], Giuseppe Tito Aronica[14], Ognjen Bonacci[15], Ivan Čanjevac[16], Andras Csik[17], Natalia Frolova[18], Boglarka Gnandt[17], Zoltan Gribovszki[19], Ali Gül[20], Knut Günther[21], Björn Guse[21,22], Jamie Hannaford[23,24], Shaun Harrigan[25], Maria Kireeva[18], Silvia Kohnová[26], Jürgen Komma[1], Jurate Kriauciuniene[27], Brian Kronvang[28], Deborah Lawrence[29], Stefan Lüdtke[21], Luis Mediero[30], Bruno Merz[21,31], Peter Molnar[32], Conor Murphy[24], Dijana Oskoruš[33,34], Marzena Osuch[35], Juraj Parajka[1], Laurent Pfister[36], Ivan Radevski[37], Eric Sauquet[38], Kai Schröter[39], Mojca Šraj[40], Jan Szolgay[26], Stephen Turner[23], Peter Valent[1], Noora Veijalainen[41], Philip J. Ward[42,43], Patrick Willems[44], Nenad Zivkovic[45].

Affiliations

[1]Institute of Hydraulic Engineering and Water Resources Management, Technische Universität Wien, Vienna, Austria.

[2]Czech Hydrometeorological Institute, Prague, Czechia.

[3]Department of Land, Environment, Agriculture and Forestry, University of Padova, Padua, Italy

[4]Department of Civil, Chemical, Environmental and Materials Engineering (DICAM), Università di Bologna, Bologna, Italy.

[5]Department of Agricultural Sciences, University of Naples Federico II, Naples, Italy.

[6]Department of Environment, Land and Infrastructure Engineering (DIATI), Politecnico di Torino, Turin, Italy.

[7]Climate Research Laboratory, Institute for Nature Management, The National Academy of Science of Belarus, Minsk, Belarus.

[8]Department of Hydrological Research, Ukrainian Hydrometeorological Institute, Kyiv, Ukraine.

[9]Department of Physical Geography and Geoecology, Faculty of Science, Charles University, Prague, Czechia.

[10]University of Architecture, Civil Engineering and Geodesy, Sofia, Bulgaria.

[11]Hydrometeorological Institute, Odessa State Environmental University, Odessa, Ukraine.

[12]Department of Engineering, University Roma Tre, Rome, Italy.

[13]Swedish Meteorological and Hydrological Institute, Norrköping, Sweden.

[14]Department of Engineering, University of Messina, Messina, Italy.

[15]Faculty of Civil Engineering, Architecture and Geodesy, Split University, Split, Croatia.

[16]Department of Geography, Faculty of Science, University of Zagreb, Zagreb, Croatia.

[17]General Directorate of Water Management, Budapest, Hungary.

[18]Department of Land Hydrology, Lomonosov Moscow State University, Moscow, Russia.

43   [19]University of Sopron, Faculty of Forestry, Institute of Geomatics and Civil Engineering, Sopron, Hungary.

44   [20]Department of Civil Engineering, Faculty of Engineering, Dokuz Eylul University, Izmir, Turkey.

45   [21]Helmholtz Centre Potsdam, GFZ German Research Centre for Geosciences, Section Hydrology, Potsdam,
46   Germany.

47   [22]Department of Hydrology and Water Resources Management, Institute for Natural Resource Conservation, Kiel
48   University, Kiel, Germany

49   [23]Centre for Ecology and Hydrology, Wallingford, UK.

50   [24]Irish Climate Analysis and Research Units (ICARUS), Department of Geography, Maynooth University,
51   Maynooth, Ireland.

52   [25]Forecast Department, European Centre for Medium-Range Weather Forecasts (ECMWF), Reading, UK.

53   [26]Department of Land and Water Resources Management, Faculty of Civil Engineering, Slovak University of
54   Technology in Bratislava, Bratislava, Slovakia.

55   [27]Lithuanian Energy Institute, Kaunas, Lithuania

56   [28]Department of Ecoscience, Danish Centre for Environment and Energy, Aarhus University, Aarhus, Denmark.

57   [29]Norwegian Water Resources and Energy Directorate, Oslo, Norway.

58   [30]Department of Civil Engineering: Hydraulic, Energy and Environment, Universidad Politécnica de Madrid,
59   Madrid, Spain.

60   [31]Institute of Environmental Sciences and Geography, University Potsdam, Potsdam, Germany

61   [32]Institute of Environmental Engineering, ETH Zurich, Zurich, Switzerland.

62   [33]Department of Hydrotechnics, Faculty of Geotechnical Engineering, University of Zagreb, Varaždin, Croatia.

63   [34]Croatian Meteorological and Hydrological Service, Zagreb, Croatia.

64   [35]Department of Hydrology and Hydrodynamics, Institute of Geophysics Polish Academy of Sciences, Warsaw,
65   Poland.

66   [36]Luxembourg Institute of Science and Technology (LIST), Esch-sur-Alzette, Luxembourg.

67   [37]Institute of Geography, Faculty of Natural Sciences and Mathematics, Ss. Cyril and Methodius University,
68   Skopje, North Macedonia.

69   [38]Irstea, UR RiverLy, Lyon-Villeurbanne, France.

70   [39]Leichtweiss Institute for Hydraulic Engineering and Water Resources, Technische Universität Braunschweig,
71   Braunschweig, Germany.

72   [40]Faculty of Civil and Geodetic Engineering, University of Ljubljana, Ljubljana, Slovenia.

73   [41]Finnish Environment Institute, Helsinki, Finland.

74   [42]Institute for Environmental Studies (IVM), Vrije Universiteit Amsterdam, The Netherlands.

75   [43]Deltares, Delft, The Netherlands.

76   [44]Department of Civil Engineering, KU Leuven, Leuven, Belgium.

77   [45]Faculty of Geography, University of Belgrade, Belgrade, Serbia.

78   [*]Corresponding author. E-mail: bertola@hydro.tuwien.ac.at

79

80

Abstract

Megafloods that far exceed previously observed records often take citizens and experts by surprise, resulting in extremely severe damage and loss of life. Existing methods based on local and regional information rarely go beyond national borders and cannot predict these floods well because of limited data on megafloods, and because flood generation processes of extremes differ from those of smaller, more frequently observed events. Here we analyse river discharge observations from over 8000 gauging stations across Europe and show that recent megafloods could have been anticipated from those previously observed in other places of Europe. Almost all observed megafloods (95.5%) fall within the envelope values estimated from previous floods at other similar places on the continent, implying that local surprises are not surprising at the continental scale. This holds also for older events, indicating that megafloods have not changed much in time relative to their spatial variability. The underlying concept of the study is that catchments with similar flood generation processes produce similar outliers. It is thus essential to transcend national boundaries and learn from other places across the continent to avoid surprises and save lives.

Main Text

Megafloods that are much larger than floods experienced previously in a given catchment or region, can take citizens and local flood managers by surprise, resulting in catastrophic damage and loss of life. For example, the discharge of the July 2021 flood at the Rhine tributaries in Germany, and rivers in the Netherlands, Belgium and Luxembourg, was up to four times larger than any event on record in the region[1], causing almost 200 fatalities and damage in excess of $40 billion. In this and other cases, the lack of previous local experience of events of this magnitude resulted in insufficient flood defence measures, preparedness and real-time response[1,2].

Because of their rare occurrence, megafloods are difficult to predict. The standard method of estimating the magnitude of potential large floods consists of fitting a probability distribution to long series of flood observations, and extrapolating the distribution to small probabilities[3]. However, long series that include several exceptional events are rarely available. Some estimation methods use flood observations from neighbouring catchments[4], to make up for the brevity of streamflow records which, however, rarely increases the chances of capturing megafloods. Even when such events are observed, accurate discharge estimates are difficult to obtain as the flood wave may partially bypass the gauge and difficulties with extrapolating the rating curve. Moreover, the processes that generate extreme floods tend to differ from those that generate smaller and more frequent events[5], making extrapolation notoriously inaccurate. One way of capturing changing flood processes with magnitude is through rainfall-runoff models, but they require long series of precipitation and are also subject to uncertainty[6,7,8]. Large floods in historic or prehistoric times

122 (paleofloods) can also be used, although the information available is often not
123 commensurate with the requirements of flood management[9,10,11].

124 An alternative for enhancing the accuracy of megaflood estimates is the transfer of
125 flood information from hydrologically similar catchments where large events may have
126 occurred[4]. In Europe the occurrence of megafloods is well documented at the national
127 scale. The August 2002 flood in Germany, Austria and Bohemia was the largest in the
128 last half century based on economic losses; the November 1994 Piedmont flood was
129 the second costliest event in Europe between 1970 and 2020[12]. Both events were
130 caused by rainfall greater than one-third of the annual total, delivered in only 72
131 hours[13,14]. However, flood information transfer rarely goes beyond national borders,
132 and no previous study has examined megafloods in a systematic way across an entire
133 continent, with the objective of learning from other places about the potential of future
134 flood surprises. Some examples comparing the world's maximum measured floods
135 also exist[15], but they do not compare hydrologically similar catchments, which makes
136 flood estimation less useful for practical proposes.

137

Anticipating megafloods

139 Here we analyse the most comprehensive dataset of annual maximum discharges in
140 Europe available to date and show that recent megafloods could have been
141 anticipated from observations in other parts of Europe, which would not be possible
142 using national data only. We also show that the predictability of megafloods does not
143 change in time when sub-periods are analysed. We base our analysis on annual
144 maximum river discharge observations from 8023 gauging stations for the period
145 1810–2021. The average length of the series is 51.4 years and the catchment areas
146 range between 1 km² and 800,000 km². Catchments across Europe are grouped into
147 five hydroclimatic regions (Fig. 1) as a first step of identifying hydrologically similar
148 catchments[16]. For each region, we estimate a regional envelope curve of flood
149 discharges that represents the relationship between flood discharge and catchment
150 area that is not exceeded by any observed flood in the region (see Methods; Extended
151 Data Table 2). To examine possible changes in time, we also compare envelope
152 curves obtained using observations from two 30-year sub-periods, i.e., 1961-1990 and
153 1991-2020.

154 We focus on 498 catchments ("target" catchments) where 510 recent (i.e. after 1999)
155 megafloods that are surprising based on local data are identified (see Methods). To
156 evaluate the possibility of anticipating megafloods in target catchments using
157 information from other places in Europe, we perform a hindcast experiment of
158 predicting their peak discharge with regional envelope curves, using flood
159 observations from similar catchments up to the year before their occurrence. For each
160 target catchment, a group of similar catchments ("donor" catchments) is identified in
161 the corresponding hydroclimatic region based on the similarity of catchment area and
162 the mean and coefficient of variation of the truncated flood series (up to the year before
163 the megaflood). From this group of donor catchments we construct an envelope curve

164 which we compare with the megaflood that occurred later in the target catchments.
165 We repeat this analysis for all 510 detected megafloods in the target catchments.

166

167 **European envelope curves of flood discharges**

168 Our data show that recent megafloods have occurred in all regions of Europe, although
169 they are more frequent in the Atlantic and Continental regions (Fig.1; Extended Data
170 Table 3), where respectively 8.7% and 7.2% of the catchments exhibit recent
171 megafloods. In the Boreal region, the respective value is only 1.3%. The smaller value
172 is related to the smaller interannual variability of floods in the Boreal region[17].

173 In the Atlantic region, the megafloods (coloured points in Fig. 1b-f) are on average 3.4
174 times larger than the local mean annual maximum discharges (squares), while in the
175 Continental and Mediterranean regions they are 5.3 and 5.2 times larger (Extended
176 Data Table 3). The larger ratio in the Mediterranean is likely related to the more non-
177 linear rainfall-runoff process and more variable precipitation in arid than in humid
178 climates[5,18]. However this analysis is not able to conclude whether megafloods are
179 becoming more frequent or not.

180 The envelope curves defined by the largest floods also differ between hydroclimatic
181 regions in terms of their intercept and slope (thick continuous lines in Fig. 1b-f;
182 Extended Data Table 2). For a catchment size of 1000 km², the envelope specific
183 discharge in the Mediterranean region is 5.26 $m^3s^{-1}km^{-2}$ while in the Boreal region it is
184 1.37 $m^3s^{-1}km^{-2}$. This is because the flood-inducing rainstorms in the Mediterranean
185 are associated with much larger intensities than the flood-inducing snowmelt typical of
186 Northern Europe. The slopes of the envelope curves are steepest in the Mediterranean
187 area (-0.57) and flattest (-0.07) in the Boreal region (Fig. 1). This is because the
188 Mediterranean rainstorms tend to be more localised than the snowmelt in the North of
189 Europe. The envelope curves for the most recent sub-period (thin dotted lines) tend to
190 be slightly lower than those for the first sub-period (thin dashed lines), except for the
191 Mediterranean and the Atlantic region. The median regression curves (thin continuous
192 lines) are slightly flatter than the respective envelopes, as larger catchments tend to
193 have more regular flood regimes than small ones. Figs. 1g-j illustrate examples of flood
194 series in pairs of catchments with and without megafloods.

195 To illustrate the potential of anticipating megafloods from other places in Europe, Fig.
196 2 shows three examples. The 2002 flood in the Kamp catchment in Austria (Fig. 2a)
197 peaked at 459 m^3s^{-1} which is equivalent to a specific discharge of 0.74 $m^3s^{-1}km^{-2}$ (black
198 triangle) given the catchment area of 622 km². The envelope curve (blue line), defined
199 by the hydrologically similar catchments within the hydroclimatic region, gives a
200 specific discharge of 1.68 $m^3s^{-1}km^{-2}$. This means that, in light of European floods, the
201 Kamp was not at all surprising while for the locals it was[19]. The regional envelope
202 discharge illustrated in Fig. 2 is defined based on previously observed floods in various
203 European countries, including Bulgaria and Poland (blue circles in Fig. 2d).

The 2009 flood in the Cumbrian Derwent catchment in the UK (Fig. 2b) peaked at 0.84 $m^3s^{-1}km^{-2}$ and was 58% larger than the second largest event on record which occurred in 2005. The corresponding envelope specific discharge is 1.64 $m^3s^{-1}km^{-2}$. Much larger extremes were observed in similar catchments in Norway (Fig. 2e). The 2009 megaflood in the Derwent was itself exceeded in 2015, however this later event still lies below the envelope curve and was not as surprising as the 2009 event (11% larger)[2].

The 2021 flood in the Ahr catchment in Germany (Fig. 2c) peaked at 0.80 $m^3s^{-1}km^{-2}$, similar to the Kamp flood, with an envelope estimate of 1.57 $m^3s^{-1}km^{-2}$. For the Ahr catchment, the similar catchments making up the donor group are, in descending order of flood magnitude: the Timis in Romania, the Freiberger Mulde in Germany, the Maritsa in Bulgaria, the Ljig in Serbia, the Lausitzer Neisse in Germany, the Corrèze and Le Lot in France, the Nysa Kłodzka in Poland and the Birs in Switzerland (Fig. 3). Although each of these catchments has a specific hydrological behaviour, overall they can be considered hydrologically similar to the Ahr in terms of average climate and flood statistical properties. All of these ten catchments experienced record-breaking floods that were surprising based on previously observed events at that location, and these occurred in the period before 2021 (Fig. 3).

The analysis of Fig. 2 is repeated for all 510 recent megafloods in the target catchments in Europe (Fig. 4). In 95.5% of the target catchments, the discharge of the envelope is larger than that of the observed megaflood, suggesting that, from a European perspective, almost none of the events can be considered a regional surprise. In 9.6% of the cases, the observed megafloods are within 75% and 150% of the envelope (red points in Fig. 4a), i.e. the order of magnitude is similar. The target catchments are distributed all over Europe with a higher concentration in the West (Fig. 4b), reflecting positive trends in flood magnitudes in Western Europe[20,21] and, to some degree, the higher station density.

The prediction is also conducted for 151 and 188 catchments with 151 and 190 recent (i.e. in the last 10 years of each sub-period) megafloods in the first and second sub-period, respectively. The distribution of the ratio between observed and predicted discharge (inset of Fig. 4a) indicates that there are no substantial changes in the predictability of megafloods in time. The discharge of the envelope is larger than that of the observed megaflood in 92% and 93.7% of the respective target catchments.

To evaluate the suitability of the donor selection, we compare the timing within the year of the target megafloods with that of the ten largest floods in the donor catchments (Fig. 4c). Flood timing is a proxy of flood generation processes[22]. Fig. 4c shows that the timing of the target megafloods (black lines) generally agrees with that of the donors (brown lines), both in terms of the average timing (angle from the centre of the circle) and the consistency of timing between events (distance to the centre). The agreement points towards the plausibility of the donor selection and prediction. A tendency for the observed timings to be more bimodal than the predictions is likely related to the smaller number of events.

Implications of expanding the perspective

Whereas previous studies have assessed the potential for megafloods mainly based on local or regional data, this study expands the observation area to the continental scale. We use megafloods that have occurred in hydrologically similar catchments elsewhere on the continent as a surrogate for the megafloods that could happen in the catchment of interest in the future.

The degree to which this transfer of information is possible depends on the suitable choice of donor catchments based on the notion of hydrological similarity[23]. The underlying concept is that catchments with similar flood generation processes, including rainfall, infiltration and flow paths, produce similar outliers, as these processes determine the transition from smaller to larger events[5,24,25]. Here we use catchment area and the mean and coefficient of variation of the truncated flood series within the same hydroclimatic region as a proxy of similarity in flood generation processes. While other similarity measures exist[16], our donor catchment selection is deemed plausible because of the similarity of the timing within the year of the events, given that timing is a fingerprint of the interplay between climatic and catchment processes[22]. Additional spot testing of catchment pairs (such as the Ahr catchment in Germany paired with the Timis catchment in Romania) based on prior knowledge from the literature[1,25] confirms the similarity. To assess robustness of the method we conduct a sensitivity analysis on the parameters of the similarity criteria and the choice of hydroclimatic regions (Extended Data Fig. 1-8). The results show that changing parameters and/or regions may modify individual donor catchments, but the envelope curve that arises from the set of donor catchments is affected much less (see method section for details).

The cross-validation experiment conducted here, starting from observed megafloods, withholding them and only using data from floods that have occurred previously, mimics the case of anticipating megafloods that have not yet occurred. We show that it is indeed feasible to estimate the order of magnitude of possible future megafloods. Almost all observed megafloods (95.5%) are smaller than the envelope values estimated, i.e. the local surprises are not surprising at the continental scale. Similar results are found for different sub-periods, indicating that megafloods have not changed much in time relative to their spatial variability within Europe. These findings are in line with recent studies in the US showing little evidence for temporal trends of large floods[26].

The proposed envelope curve approach complements alternative methods such as regional statistical approaches that spatially interpolate observed discharges[4] or process-based rainfall-runoff modelling[27]. These methods provide best estimates of expected floods, while the envelope method reflects a possible worst case – which itself is an important aspect of flood risk planning.

The focus on a possible worst case implies that the envelope values are generally too large to serve as design values for most types of flood defence infrastructure from a cost-benefit perspective. Rather, they describe a possibility space[28] that is prudent to consider as civil protection scenarios, required to organise local preparedness, and for testing the safety of very large dams. They can be used to derive extreme flood hazard scenarios, either failure scenarios (what can go wrong?) or future development scenarios (what could the future look like?) that could strengthen existing methods such as the Probable Maximum Flood (PMF) concept[29]. There is an increasing need for considering the extremes of the extremes, as there is a tendency in society for smaller acceptable risks[29], so flood risk management should account for the potential of surprises and their devastating consequences. This requires a shift in thinking[29] and the application of envelope curves, storylines[2,30] and compound event analyses[31]. Making individuals and societies more robust against surprises therefore goes beyond the design of spillways and flood management plans.

In summary, to anticipate megafloods we must learn from other places in order to reduce the surprise factor of their occurrence, increase flood risk awareness and enhance preparedness of flood risk management. To this end, it is essential to move beyond national flood risk assessment and share information on megafloods across countries and continents.

Acknowledgements

Author Contributions Statement

Competing Interests Statement

The authors declare no competing interests.

Figure Captions
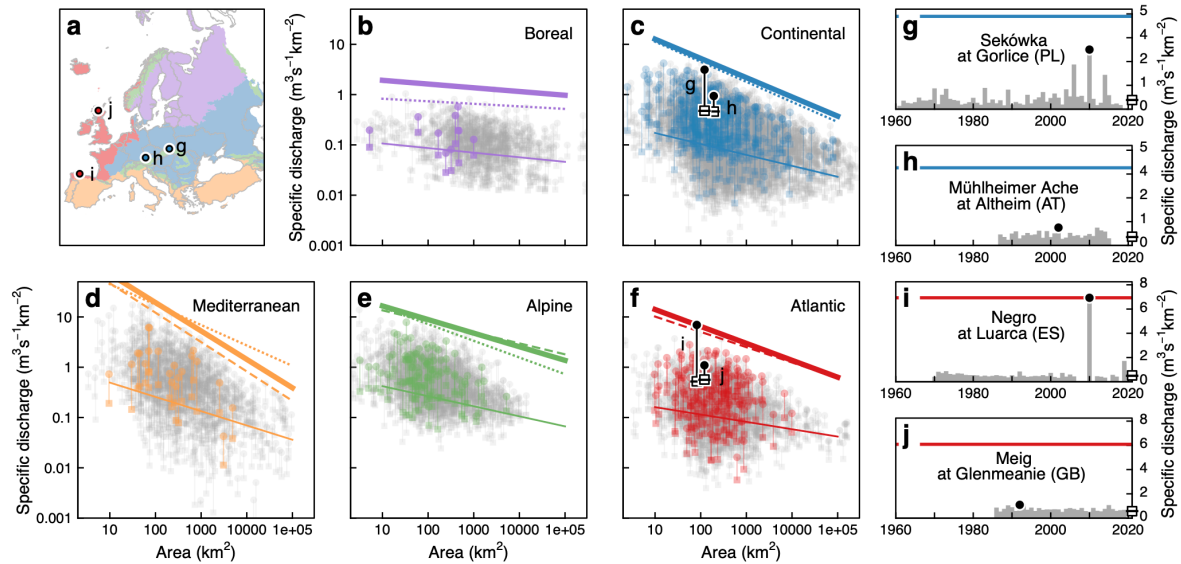
Fig. 1: Megafloods in Europe. (a) Five hydroclimatic regions: Boreal (purple), Continental (blue), Mediterranean (orange), Alpine (green) and Atlantic (red). (b-f) Maximum observed specific flood discharges (points) and mean of annual specific flood discharges (squares) over the entire observation period at each stream gauge as a function of catchment area. Regional envelope curves (thick lines) and median regional annual specific flood discharges (thin lines) for the full record period are shown for each hydroclimatic region. Envelope curves for two 30-year sub-periods are also shown (dashed lines for 1961-1990, dotted lines for 1991-2020). Parameters of the envelope curves are listed in Extended Data Table 2. Coloured symbols indicate the mean and maximum flood discharges in the 498 catchments with recent megafloods, grey points those of the remaining catchments. (g-j) Examples of series of annual flood discharges with (g and i) and without (h and j) megafloods; their corresponding mean (squares) and maximum values (points) are highlighted in black in (c) and (f). The locations of corresponding stream gauges are indicated in (a) by circles.
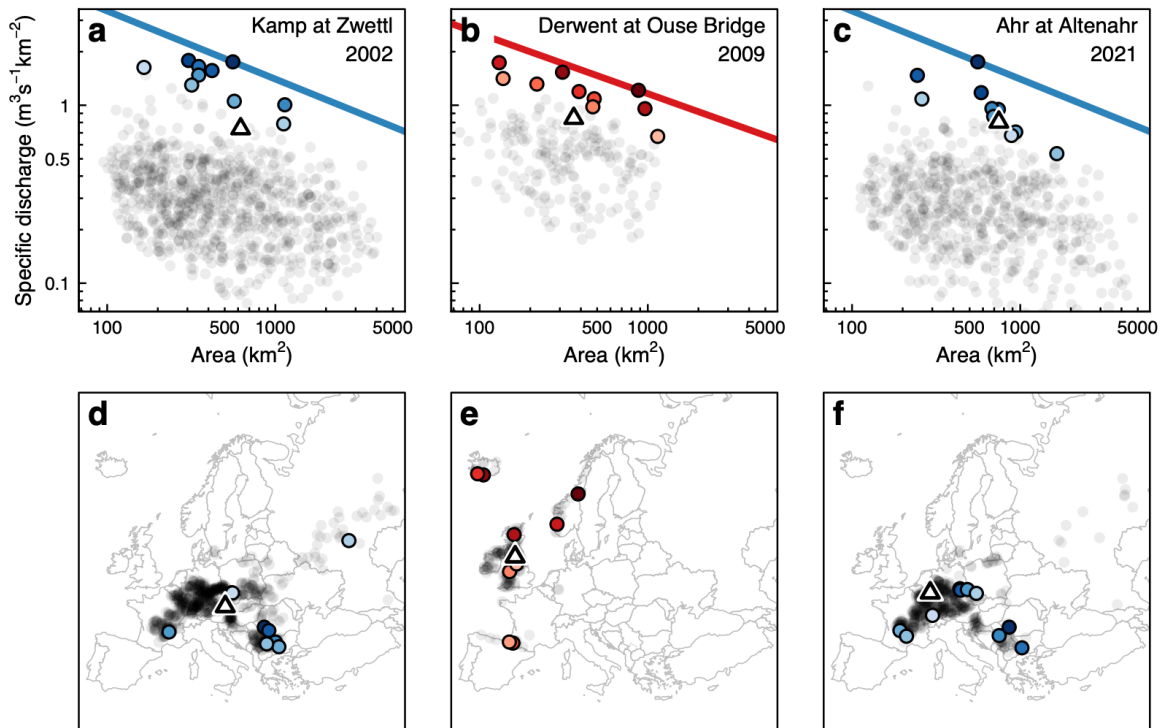
Fig. 2: Envelope curves for three catchments with recent megafloods in Europe.
(a,d) Kamp (622 km² catchment area) with 2002 flood; (b,e) Cumbrian Derwent (363 km²) with 2009 flood, and (c,f) Ahr (746 km²) with 2021 flood, indicated with triangles. (a-c) Maximum specific discharges observed before the year of occurrence of the megaflood for 824 (a), 196 (b) and 590 (c) similar donor catchments (points) selected within the corresponding hydroclimatic region. Coloured points indicate ten largest events (in terms of distance to the envelope curve), with shades being darker for events that are closer to the envelope. Line shows resulting envelope curve with the slope estimated from the hydroclimatic regions (Fig. 1b-f). (d-f) Location of the target (triangle) and donor (points) catchments. Note that the envelope curves of Fig. 1 refer to the entire hydroclimatic region, while here they refer to the donor group within a region.

368
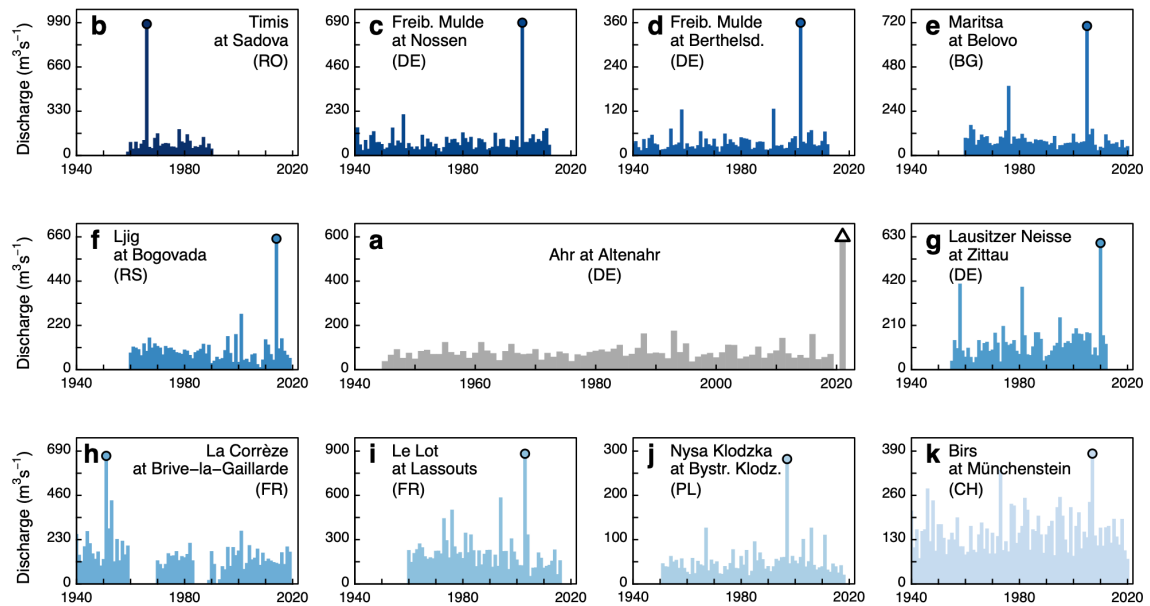
Fig. 3: Annual flood series for the Ahr and ten donor catchments with extreme floods. (a) Ahr at Altenahr, Germany, with 2021 megaflood (the target event) indicated as a triangle. (b-k) Series for the ten donor catchments indicates as coloured dots in Fig. 2c,f).

373

374
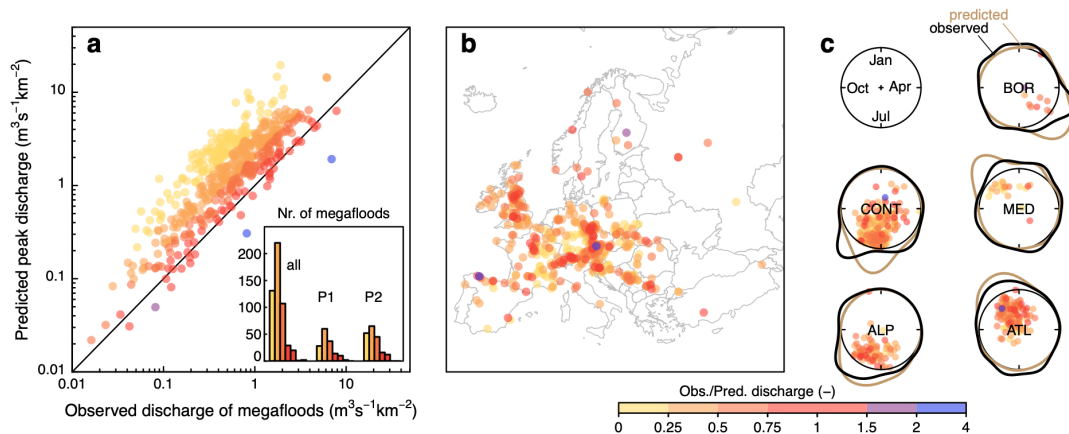
Fig. 4: Predicted versus observed megafloods. (a) Predicted specific envelope discharge for 498 target catchments versus observed specific discharge of the megafloods in the same catchments. Predicted envelope discharges are estimated using discharge observations from a pool of donor catchments up to the year before the target megaflood. The number of target megafloods is shown in the inset for the entire period ("all") and the two sub-periods 1961-1990 ("P1") and 1991-2020 ("P2"). Colours indicate the ratio of observed and predicted discharge. (b) Location of target catchments. Megafloods occur all over Europe and are less surprising than commonly assumed. (c) Circular distribution of the timing of the megafloods observed in the

target catchments (black lines), and mean timing of the 10 largest floods in the donor catchments (coloured points) and their distribution (brown lines). The distance of the points to the centre is inversely proportional to the standard deviation of the flood timing.

References

1. Apel, H., Vorogushyn, S., & Merz, B. Brief communication–Impact Forecasting Could Substantially Improve the Emergency Management of Deadly Floods: Case Study July 2021 floods in Germany. Natural Hazards and Earth System Sciences Discussions, 1-10 (2022).

2. Kreibich, H., Van Loon, A.F., Schröter, K. et al. The challenge of unprecedented floods and droughts in risk management. Nature 608, 80–86 (2022).

3. De Niel, J., Demarée, G., Willems, P. Weather typing based flood frequency analysis validated for exceptional historical events of past 500 years along the Meuse river, Water Resources Research, 53(10), 8459-8474 (2017).

4. Robson, A. J. and Reed, D. W. Flood Estimation Handbook (FEH), chap. Statistical procedures for flood frequency estimation, p. Vol. 3, Institute of Hydrology, Wallingford, UK (1999).

5. Rogger, M., Pirkl, H., Viglione, A., Komma, J., Kohl, B., Kirnbauer, R., Merz, R., & Blöschl, G. (2012). Step changes in the flood frequency curve: Process controls. Water Resources Research, 48(5), 1–15.

6. Bergstrand M., Asp S. and Lindström G. Nationwide hydrological statistics for Sweden with high resolution using the hydrological model S-HYPE. Hydrology Research, 45.3, 349-356 (2014).

7. Devitt, L., Neal, J., Wagener, T., & Coxon, G. Uncertainty in the extreme flood magnitude estimates of large-scale flood hazard models. Environmental Research Letters, 16(6), 064013 (2021).

8. Bouaziz, L. et al. Behind the scenes of streamflow model performance, Hydrol. Earth Syst. Sci., 25, 1069–1095 (2021).

9. Kjeldsen, T.R. et al. Documentary evidence of past floods in Europe and their utility in flood frequency estimation. Journal of Hydrology, 517, 963–973 (2014).

10. Blöschl, G., Kiss, A., Viglione et al. Current European flood-rich period exceptional compared with past 500 years. Nature, 583(7817), 560–566 (2020).

11. U.S. Geological Survey Scientific Investigations Report 2020–5065, 89 p. (2020).

12. World Meteorological Organisation (WMO). WMO Atlas of Mortality and Economic Losses from Weather, Climate and Water Extremes (1970–2019). WMO-No. 1267 (2021).

13. Blöschl, G., Nester, T., Komma, J., Parajka, J., & Perdigão, R. A. P. The June 2013 flood in the Upper Danube Basin, and comparisons with the 2002, 1954 and 1899 floods. Hydrology and Earth System Sciences, 17(12), 5197–5212 (2013).

14. Lionetti, M. The Italian floods of 4–6 November 1994. *Weather*, *51*(1), 18-27 (1996).

15. Herschy, R. W. (2002). The world's maximum observed floods. Flow Measurement and Instrumentation, 13(5–6), 231–235. https://doi.org/10.1016/S0955-5986(02)00054-7

16. Kuentz, A., Arheimer, B., Hundecha, Y., and Wagener, T. Understanding hydrologic variability across Europe through catchment classification, Hydrol. Earth Syst. Sci., 21, 2863-2879 (2017)

426 17. Lun, D., Viglione, A., Bertola, M., Komma, J., Parajka, J., Valent, P., & Blöschl, G. Characteristics
427   and process controls of statistical flood moments in Europe – a data-based analysis. Hydrology
428   and Earth System Sciences, 25(10), 5535–5560 (2021).

429 18. Blöschl, G. Flood generation: process patterns from the raindrop to the ocean, Hydrol. Earth Syst.
430   Sci., 26, 2469–2480 (2022)

431 19. Blöschl, G. Flood warning - on the value of local information. International Journal of River Basin
432   Management, 6 (1), pp. 41-50 (2008).

433 20. Blöschl, G., Hall, J., Viglione, A. et al. Changing climate both increases and decreases European
434   river floods. Nature, 573(7772), 108–111 (2019).

435 21. Bertola, M., Viglione, A., Lun, D., Hall, J., & Blöschl, G. Flood trends in Europe: are changes in
436   small and big floods different? Hydrology and Earth System Sciences, 24(4), 1805–1822 (2020).

437 22. Blöschl, G., Hall, J., Parajka, J., Perdigão, R. A., Merz, B., Arheimer, B., ... & Živkoviæ, N.
438   Changing climate shifts timing of European floods. Science, 357(6351), 588-590 (2017).

439 23. Blöschl, G., Sivapalan, M., Wagener, T., Viglione, A., Savenije, H.H. Runoff Prediction in
440   Ungauged Basins – Synthesis across Processes, Places and Scales. Cambridge University Press
441   (2013).

442 24. Kemter, M., Merz, B., Marwan, N., Vorogushyn, S., & Blöschl, G. Joint Trends in Flood
443   Magnitudes and Spatial Extents Across Europe. Geophysical Research Letters, 47(7), 1–8
444   (2020).

445 25. Popescu, I., Jonoski, A., Van Andel, S. J., Onyari, E., & Moya Quiroga, V. G. Integrated modelling
446   for flood risk mitigation in Romania: case study of the Timis–Bega river basin. International journal
447   of river basin management, 8(3-4), 269-280 (2010).

448 26. Collins, M. J., Hodgkins, G. A., Archfield, S. A., & Hirsch, R. M. (2022). The occurrence of large
449   floods in the United States in the modern hydroclimate regime: Seasonality, trends, and large-
450   scale climate associations. Water Resources Research, 58,
451   e2021WR030480. https://doi.org/10.1029/2021WR030480

452 27. Donnelly, C, Andersson, J.C.M. and Arheimer, B. Using flow signatures and catchment similarities
453   to evaluate a multi-basin model (E-HYPE) across Europe. Hydr. Sciences Journal 61(2):255-273
454   (2016)

455 28. Sivapalan, M., & Blöschl, G. Time scale interactions and the coevolution of humans and water.
456   Water Resources Research, 51(9), 6988–7022 (2015).

457 29. Merz, B., Vorogushyn, S., Lall, U., Viglione, A., & Blöschl, G. Charting unknown waters-On the
458   role of surprise in flood risk assessment and management. Water Resources Research, 51(8),
459   6399–6416 (2015).

460 30. Shepherd, T. G. Storyline approach to the construction of regional climate change information.
461   Proceedings of the Royal Society A, 475(2225), 20190013 (2019).

462 31. Thieken, A. H., Samprogna Mohor, G., Kreibich, H., and Müller, M.: Compound inland flood
463   events: different pathways, different impacts and different coping options, Nat. Hazards Earth
464   Syst. Sci., 22, 165–185 (2022).

465

Methods

Datasets

The hydrological data used in this study were obtained from a pan-European Flood Database[32] with subsequent updates. The current version contains data from 8,023 hydrometric gauging stations from 68 European data sources for the period 1810–2021 (Extended Data Table 1). The dataset consists of the highest discharge (daily mean or instantaneous discharge) in each calendar year for each station. The stations are located within the domain bounded by 22.25° W–63.25° E and 34.25° N–71.25° N (Extended Data Fig. 1), and catchment areas range between 1 km^2 and 800,000 km^2. The dataset was screened for data errors. The screening involved visual examination of the flood records, analysis of flood seasonality and examination of the guage location and catchment area in Google Maps. All available stations, including those affected by reservoir construction, were considered for the analysis because reservoir effects were deemed to have little significance for envelope curves for large hydroclimatic regions. Similarly, all available years with data were considered notwithstanding differences in the record lengths, because the focus was on the maxima observations of each series. The minimum series length is 10 years, and the average length is 51.4 years.

The gauging stations were grouped into five regions (Fig. 1a; Extended Data Fig.1) that reflect similar hydroclimatic conditions by generalising the European Biogeographical regions[33] with a view on flood processes. The Steppic and Pannonian regions were merged with the Continental region, the Arctic region with the Boreal region, and the Anatolian and Black Sea regions with the Mediterranean region. Additionally, part of northern Italy was considered as part of the Mediterranean region and Iceland as part of the Atlantic region. For comparison, an alternative subdivision of Europe into five regions[17] was considered in a sensitivity analysis (Extended Data Fig. 4a). In order to examine possible changes, the observation period was subdivided into two 30-year sub-periods, P1 (1961-1990) and P2 (1991-2020).

Regional envelope curves

We quantified the largest flood events in each region by scaling the peak discharges by catchment area via envelope curves that represent the upper limit of the dataset (Fig. 1):

$$log(q) = a + b \cdot log(A) \qquad (1)$$

where q (m^{3}s^{-1}km^{-2}) is the specific discharge, i.e. the discharge per unit catchment area A. The parameter b was estimated by quantile regression with quantile z=0.999 using the rq function of the R quantreg package[34,35]. The quantile regression enables a more robust estimate than the tangents on the maxima, because it uses the complete dataset rather than the maxima only. The intercept a was determined such that it

506 satisfies the envelope condition, i.e. the envelope curve is the upper bound of all
507 observed flood discharges in a region (Extended Data Table 2). For comparison, a
508 quantile regression with z=0.5 is also shown in Fig. 1 (thin line).
509

510 **Megafloods**

511 For the selection of recent megafloods (Fig. 4) the following criteria were adopted:
512 (i) the discharge value is a high outlier in the corresponding series of annual maximum
513 flood discharges, according to the definition[36]:

514
$$q_{mf} > Q_3 + k * (Q_3 - Q_1) \qquad (2)$$

515 where Q_1 and Q_3 are the first and third quartile (i.e. respectively 25% and 75% of the
516 observations lies below this values) and k=3;

517 (ii) the discharge value is record-breaking and locally surprising, i.e., its return period
518 T_{mf} is at least 3 times larger than the return period of the second largest event up to
519 that year T_{sl}. The return period was obtained by fitting a GEV distribution to each flood
520 series up to the year of the megaflood using the L-moments (R extRemes package).

521 (iii) it occurred after the year 1999 (when the full observation period is analysed) and
522 the corresponding series has at least 20 years of data previous to the event.

523 The selection resulted in a set of 510 megafloods from 498 target catchments, whose
524 observed specific discharge and location of corresponding gauges are shown in Fig.
525 4a and 4b. When detecting megafloods in the two 30-year sub-periods, only
526 observations within each sub-period are considered and the criterion (iii) is modified
527 such that events in the last 10 years of the respective sub-period are selected (i.e.
528 after 1979 for P1 and after 2009 for P2).

529 We tested the robustness of the results to the criterion (i) for the selection of high
530 outliers, using the definition for skewed data[37]:

531
$$\begin{cases} q_{mf} > Q_3 + 1.5e^{3MC}IQR & if \ MC > 0 \\ q_{mf} > Q_3 + 1.5e^{4MC}IQR & if \ MC < 0 \end{cases} \qquad (3)$$

532 Where MC is the medcouple[38], a robust measure of skewness, defined as:

533
$$MC(X_n) = \operatorname*{med}_{x_i \leq m_n \leq x_j} h(x_i, x_j) \qquad (4)$$

534 with m_n is the sample median of X_n and

535
$$h(x_i, x_j) = \frac{(x_j - m_n) - (m_n - x_i)}{x_j - x_i} \qquad (5)$$

536 The alternative selection resulted in a set of 677 megafloods (Supplementary Fig. S1),
537 whose observed specific discharge and location of corresponding gauges are shown
538 in Supplementary Fig. S2.

539 We also tested the sensitivity of the results to criterion (ii) for the selection of record-
540 breaking and surprising events, by varying the threshold T_{mf}/T_{sl} between 1 and 4. The
541 results of the sensitivity analysis are shown in Supplementary Fig. S3 and indicate
542 that, when the definition of megafloods is extended to less surprising events (i.e. T_{mf}/T_{sl}
543 <3), the fraction of megaflooods larger than the envelope is unchanged. The only
544 exception is the Boreal region, where fewer events are selected.

545

Donor catchments

547 For each catchment in which a megaflood had occurred (target catchment), a pool of
548 similar catchments (donor catchments) was identified in the same region. The
549 similarity between the catchments was quantified in terms of weighted normalised
550 Euclidean distance D in a three-dimensional space with the following dimensions: the
551 logarithm of catchment area A, the logarithm of the mean of the annual maximum
552 specific discharges q_m normalised to a catchment area of 100km^2, and the coefficient
553 of variation CV of the annual maximum discharges:

$$D = \sqrt{\alpha \left(\frac{\log A_i - \log A_j}{sd(\log A)}\right)^2 + \beta \left(\frac{\log q_{m,i} - \log q_{m,j}}{sd(\log q_m)}\right)^2 + \gamma \left(\frac{CV_i - CV_j}{sd(CV)}\right)^2} \quad (6)$$

555 where i refers to the target catchment, j to a potential donor catchment and sd is the
556 standard deviation of all catchments in the donor group. Greek letters indicate weights.
557 q_m and CV were calculated on flood data prior to the year of occurrence of the target
558 event to obtain a cross-validation experiment that resembles a case of anticipating
559 megafloods a priori. In estimating q_m and CV we excluded outliers (for both the target
560 and the donor catchments) according to the criterion of Eq. (2), because megafloods
561 should not influence the comparison, and only smaller, frequently occurring floods
562 were used, which is the only information usually available in the case of a prediction.
563 In selecting the number of catchments in the pooling group, there is a tradeoff between
564 a larger group that has a higher chance of containing very large floods, and a smaller
565 group that is hydrologically more homogeneous. For Fig. 1, 2, 3 we used $\alpha=\beta=\gamma=1$
566 (corresponding to the assumption of the three dimensions having the same
567 importance) and included catchments with $D<D_{max}$ with $D_{max}=1$, guided by a sensitivity
568 analysis (see below and Extended Data Fig. 2).

569

Megaflood prediction

571 We repeated the selection of the donor group for each target catchment and estimated
572 the envelope curve, using the slope b of the corresponding hydroclimatic region and
573 the intercept determined as the minimum that satisfies the envelope condition of the
574 group only. The procedure only uses observations from donor catchments up to the
575 year before the megaflood in the target catchment (Fig. 2a-c). We finally obtained an
576 estimate of the discharge of a potential megaflood in the target catchment (predicted

577 megaflood) from the envelope curve and compared it to the discharge of the observed
578 megaflood (Fig. 4a).

579 In order to evaluate the plausibility of the donor selection we analysed the timing of
580 the megafloods observed in the target and donor catchments using previously
581 established methods[22] (Fig. 4c). We compared the distribution of the timing of the
582 observed megafloods to the average timing of the 10 largest floods in the donor group.
583 The circular distributions in Fig. 4c were obtained using the R circular package.

584

585 In order to evaluate the robustness of the method we conducted a number of sensitivity
586 analyses. We varied D_{max} between 0.5 and 1.5 and showed that an increase in D_{max}
587 translates into an increasing number of target megafloods that are below the envelope
588 (Extended Data Fig. 2). The larger fraction in the Boreal region is because of fewer
589 donors available compared to the other regions. We also tested the sensitivity of α, β
590 and γ, examining four weight combinations: equal weights ($\alpha=\beta=\gamma=1$) and doubling
591 one of the weights ($\alpha=2$ and $\beta=\gamma=1$; $\alpha=\gamma=1$ and $\beta=2$; $\alpha=\beta=1$ and $\gamma=2$), which
592 corresponds to the hypothesis of one dimension being more important than the others
593 in the donor selection. There is very little effect on the number of target megafloods
594 below the envelope (Extended Data Fig. 3). While a different set of parameters may
595 modify some of the donor catchments, the resulting envelope curve changes very little.
596 Finally we tested the effect of replacing the regional subdivision of Fig. 1 by an
597 alternative subdivision[17]. The analysis shows that the alternative regions may modify
598 the choice of individual donor catchments but, again, the overall conclusions do not
599 change (Extended Data Fig. 4-7).
600

Data availability

602 The flood discharge data from the data holders/sources listed in Extended Data
603 Table 1 that were used in this paper are available at
604 https://github.com/tuwhydro/megafloods.

605

Code availability

607 The data analysis was performed in R using the supporting packages circular,
608 lubridate, plotrix, quantreg, raster, RColorBrewer, rgdal, rworldmap and scales. The
609 code used can be downloaded from https://github.com/tuwhydro/megafloods.

610

Methods-only references

612 32. Hall, J. et al. A European Flood Database: facilitating comprehensive flood research beyond
613 administrative boundaries. Proc. Int. Assoc. Hydrol. Sci. 370, 89–95 (2015)

33. Roekaerts, M.: The biogeographical regions map of Europe, in: Basic principles of its creation and overview of its development, European Environment Agency, Copenhagen, available at: https://www.eea.europa.eu/data-and-maps/ data/biogeographical-regions-europe-3 (2002).

34. Koenker, R. W. Quantile Regression, Cambridge U. Press (2005).

35. Amponsah, W., Marra, F., Marchi, L., Roux, H., Braud, I., Borga, M. Objective Analysis of Envelope Curves for Peak Floods of European and Mediterranean Flash Floods. In: Leal Filho, W., Nagy, G., Borga, M., Chávez Muñoz, P., Magnuszewski, A. (eds) Climate Change, Hazards and Adaptation Options. Climate Change Management. Springer, Cham (2020).

36. Tukey JW. Exploratory Data Analysis. Reading (Addison-Wesley): MA, 1977.

37. Hubert, M., & Vandervieren, E. (2008). An adjusted boxplot for skewed distributions. Computational statistics & data analysis, 52(12), 5186-5201.

38. Brys G, Hubert M, Struyf A. A robust measure of skewness. J. Comput. Graph. Stat. 2004; 13: 996–1017.